



The Poisson-Topp-Leone Burr Type- \mathcal{XII} Model: Various Uncensored Applications for Statistical Modeling and Some Copulas

Murtadha Mansour Abdullah^{1,*}, Wahhab Salim Mohammed² and Aqeel Hameed Farhana²

¹University of Wasit. College of Administration and Economics

²University of Diyala. College of Administration and Economics

Abstract The Poisson-Topp-Leone Burr type- \mathcal{XII} distribution is studied mainly for illustrating its wide applicability under uncensored engineering and medical real-life datasets. The real-life datasets are checked and analyzed for the statistical modeling purpose. The Poisson-Topp-Leone Burr type- \mathcal{XII} model is compared with other nine types of Burr type- \mathcal{XII} extensions and provided the best results. For modeling the bivariate uncensored engineering and medical real-life datasets, we presented some bivariate version with some useful theoretical results. Those versions are investigated due to certain and common copulas.

Keywords Burr type- \mathcal{XII} , Applicability, Real-life dataset, Copulas

AMS 2010 subject classifications 62N02, 62N01, 60E05, 62E10, 62G05, 62N05, 62P30

DOI: 10.19139/soic-2310-5070-1567

1. Introduction and motivation

In the statistical applications and real-life data modeling, a very special efforts has devoted for the twelve models of Burr [12]. For example, Yousof et al., [50] presented and characterized (under some characterization theorems) a new version of the zero-truncated-Burr type- \mathcal{XII} model called the Poisson-Topp-Leone Burr type- \mathcal{XII} (PTL-BR \mathcal{XII}). In their theoretical study, Yousof et al., [52] presented some theoretical results such as some characterizations and some statistical properties including the distribution of the order statistics, the moments (ordinary and incomplete), some useful life functions (residual and reversed functions) and also the function of generating moment. The cumulative distribution function (CDF) of the PTL-BR \mathcal{XII} version can be written as

$$F(z; \underline{\psi}) = \varkappa_{[\theta_1]}^{-1} \left(1 - \exp \left\{ -\theta_1 [\xi_{\theta_2}(z)^{-2\beta_2}]^{\beta_1} \right\} \right), \quad (1)$$

for all $\theta_1 \in \mathbf{R} - \{0\}$, $\theta_2 \in \mathbf{R}^+$, $\beta_1 \in \mathbf{R}^+$, $\beta_2 \in \mathbf{R}^+$, where

$$\varkappa_{[\theta_1]}^{-1} = \frac{1}{1 - \exp(-\theta_1)},$$

$$\xi_{\theta_2}(z) = 1 - (1 + z^{\theta_2}),$$

*Correspondence to: *Corresponding author: Murtadha Mansour Abdullah (Email:mabdullah@uowasit.edu.iq). University of Wasit. College of Administration and Economics.

and $\underline{\psi} = (\theta_1, \beta_1, \theta_2, \beta_2)$. The corresponding probability density function (PDF) of (1) can be derived as

$$f(z; \underline{\psi}) = 2\theta_1\beta_1\theta_2\beta_2 \kappa_{[\theta_1]}^{-1} \frac{z^{\theta_2-1} (1+z^{\theta_2})^{-2\beta_2-1} [\xi_{\theta_2}(z)^{-2\beta_2}]^{\beta_1-1}}{\exp \left\{ \theta_1 [\xi_{\theta_2}(z)^{-2\beta_2}]^{\beta_1} \right\}}. \quad (2)$$

The hazard (failure) function (HRF) of the PTL-BR $\mathcal{X}\mathcal{II}$ version can be obtained as

$$h(z; \underline{\psi}) = 2\theta_1\beta_1\theta_2\beta_2 \frac{z^{\theta_2-1} (1+z^{\theta_2})^{-2\beta_2-1} [\xi_{\theta_2}(z)^{-2\beta_2}]^{\beta_1-1}}{\exp \left\{ \theta_1 [\xi_{\theta_2}(z)^{-2\beta_2}]^{\beta_1} \right\} - 1}. \quad (3)$$

The cumulative HRF (CHRF) can be written as

$$H(z; \underline{\psi}) = -\ln \left[1 - \kappa_{[\theta_1]}^{-1} \left(1 - \exp \left\{ -\theta_1 [\xi_{\theta_2}(z)^{-2\beta_2}]^{\beta_1} \right\} \right) \right]. \quad (4)$$

When new distributions are defined, a problem of great concern for the study of inference is the identifiability of the distribution. In this work, we argue that there may be an identifiability problem in the new paradigm. Although this did not affect practical applications and statistical modeling, we must mention the reality of this problem, and we must also propose an appropriate and logical solution to it. For $\beta_1 = 1$, PTL-BR $\mathcal{X}\mathcal{II}$ model will be reduced to the reduced Poisson-Topp-Leone Burr type- $\mathcal{X}\mathcal{II}$ (RPTL-BR $\mathcal{X}\mathcal{II}$) version, this new model, this reduced model certainly does not suffer from the identification problem. Since the identification problem does not affect the applied ability of the model nor any of the mathematical and statistical modeling operations, the applications in this research were carried out based on PTL-BR $\mathcal{X}\mathcal{II}$ model. We suggest that in future work it may be appropriate to address the reduced model in some detail while presenting other suitable practical applications on real data.

The main motivation and the real justification for the PTL-BR $\mathcal{X}\mathcal{II}$ lifetime model is the fame and the celebrity of using and applying the standard Burr type- $\mathcal{X}\mathcal{II}$ (BRXII) model (see Burr [13], Burr & Cislak [15], Burr [12] and Burr [14], Tadikamalla [49] and Rodriguez [43]). Recently, Cordeiro [17] investigated a new family based on the BRXII distribution and presented a useful regression model for prediction and regression modeling.

In this article, we will focus on the applied aspects of the PTL-BR $\mathcal{X}\mathcal{II}$ model. For the bivariate modeling of the bivariate uncensored engineering and medical real-life datasets, we presented many bivariate version with some useful theoretical results. Those version are investigated due to certain and common copulas. For more Burr $\mathcal{X}\mathcal{II}$ extensions see Paranaíba et al [42] for The beta Burr $\mathcal{X}\mathcal{II}$ distribution, Paranaíba et al [41] for the Kumaraswamy Burr $\mathcal{X}\mathcal{II}$ distribution, Korkmaz et al., [26] for the odd Lindley Burr $\mathcal{X}\mathcal{II}$ distribution, Yousof et al., [52] for the Topp Leone generated Burr $\mathcal{X}\mathcal{II}$ distribution, Gad et al., [24] for The Burr $\mathcal{X}\mathcal{II}$ -Burr $\mathcal{X}\mathcal{II}$ distribution and Elsayed and Yousof [21] for the extended Poisson generalized Burr $\mathcal{X}\mathcal{II}$ distribution. Some other useful Burr $\mathcal{X}\mathcal{II}$ extensions can found in Abouelmagd et al., [1] and Abouelmagd et al., [2]. In this article, the Poisson Topp Leone Burr $\mathcal{X}\mathcal{II}$ distribution is studied in practical applications.

For this purpose, four real-life datasets are analyzed under the uncensored samples, the PTL-BR $\mathcal{X}\mathcal{II}$ lifetime distribution is compared with many Burr type- $\mathcal{X}\mathcal{II}$ distributions, and provided the best fits under the four criterion. the PTL-BR $\mathcal{X}\mathcal{II}$ lifetime distribution can be hardly recommended for mathematical, statistical modeling and analysis of the monotonically increasing failure rate and U-failure rate datasets. The PTL-BR $\mathcal{X}\mathcal{II}$ lifetime distribution can also be recommended for the bivariate (symmetric and asymmetric) datasets, the PTL-BR $\mathcal{X}\mathcal{II}$ lifetime distribution can be also recommended either it was

left skewed (symmetric and asymmetric) datasets or right skewed (symmetric and asymmetric) datasets. The PTL-BR $\mathcal{X}\mathcal{I}\mathcal{I}$ model can be used Bayesian and classical inference for the generalized stress-strength models, see Rasekhi et al., [35], Saber et al., [38], Saber et al., [39] and Saber and Yousof [37].

2. Copula

In this Section, and due to Yousof et al., [54], Ali et al., [4], Ali et al., [3], Mansour et al., ([27],[28],[29],[30], [31] and [32]) and Ali et al.,[6], we present some novel bivariate PTL-BR $\mathcal{X}\mathcal{I}\mathcal{I}$ (BPTL-BR $\mathcal{X}\mathcal{I}\mathcal{I}$) versions using

- The so called copula of Farlie, Gumbel and Morgenstern (FGM) (see Gumbel [23], Morgenstern [33] and Gumbel [22] and Elgohari & Yousof ([18], [19] for more applications).
- The modified version of Rodriguez-Lallena and Ubeda-Flores [36]).
- The copula of Clayton (see Al-babtain et al., [8] for more details).
- The entropy copula (see Pougaza and Djafari [34], Ali et al., [5] and Ali et al., [7]).

The Multivariate PTL-BR $\mathcal{X}\mathcal{I}\mathcal{I}$ (MPTL-BR $\mathcal{X}\mathcal{I}\mathcal{I}$) model is also presented.

Considering FGM model as an initial example, the joint-CDF of the FGM is

$$F_\rho(\hbar, \varpi) = \hbar\varpi(1 + \rho\hbar^*\varpi^*)|_{\hbar^*=1-\hbar, \varpi^*=1-\varpi},$$

where the functions $\hbar = F_1$ and $\varpi = F_2$ are given marginal functions and the parameter $\rho \in (-1, 1)$ is called the parameter of the dependence for every

$$\hbar \in (0, 1), \varpi \in (0, 1), 0 = F(\hbar, 0) = F(0, \varpi)$$

where "minimum-grounded" and $F(\hbar, 1) = \hbar$ and $F(1, \varpi) = \varpi$ which is "maximum-grounded" where

$$F(\hbar_1, \varpi_1) + F(\hbar_2, \varpi_2) - F(\hbar_1, \varpi_2) - F(\hbar_2, \varpi_1) \geq 0.$$

2.1. The BPTL-BR $\mathcal{X}\mathcal{I}\mathcal{I}$ via the FGM model

The FGM copula is continuous in \hbar and ϖ if

$$|F(\hbar_2, \varpi_2) - F(\hbar_1, \varpi_1)| \leq |\hbar_2 - \hbar_1| + |\varpi_2 - \varpi_1|,$$

which is the Lipschitz condition (the stronger condition of Lipschitz).

For $0 \leq \hbar_1 \leq \hbar_2 \leq 1$ and $0 \leq \varpi_1 \leq \varpi_2 \leq 1$, we have

$$\Pr(\hbar_1 \leq \hbar \leq \hbar_2, \varpi_1 \leq \varpi \leq \varpi_2) = -F(\hbar_1, \varpi_2) + F(\hbar_1, \varpi_1) - F(\hbar_2, \varpi_1) + F(\hbar_2, \varpi_2) \geq 0.$$

Setting

$$\hbar^* = 1 - F_{\underline{\psi}_1}(x_1)|_{[\hbar^*=(1-\hbar)\in(0,1)]},$$

and

$$\varpi^* = 1 - F_{\underline{\psi}_2}(x_2)|_{[\varpi^*=(1-\varpi)\in(0,1)]}.$$

Then, the corresponding joint CDF of the BPTL-BR $\mathcal{X}\mathcal{I}\mathcal{I}$ is

$$\begin{aligned} F_\rho(\hbar, \varpi) &= \varkappa_{[\theta_1]}^{-1} \left(1 - \exp \left\{ -\theta_1 \left[\xi_{\theta_2}(\hbar)^{-2\beta_2} \right]^{\beta_1} \right\} \right) \\ &\quad \times \varkappa_{[c_1]}^{-1} \left(1 - \exp \left\{ -c_1 \left[\xi_{c_2}(\varpi)^{-2b_2} \right]^{b_1} \right\} \right) \\ &= \left(1 + \rho \left\{ \begin{array}{l} \left[1 - \varkappa_{[\theta_1]}^{-1} \left(1 - \exp \left\{ -\theta_1 \left[\xi_{\theta_2}(\hbar)^{-2\beta_2} \right]^{\beta_1} \right\} \right) \right] \\ \left[1 - \varkappa_{[c_1]}^{-1} \left(1 - \exp \left\{ -c_1 \left[\xi_{c_2}(\varpi)^{-2b_2} \right]^{b_1} \right\} \right) \right] \end{array} \right\} \right), \end{aligned}$$

The joint PDF can then derived from

$$f_\rho(\hbar, \varpi) = \rho \hbar^\cdot \varpi^\cdot + 1$$

where

$$\hbar^\cdot = -2\hbar + 1$$

and

$$\varpi^\cdot = -2\varpi + 1$$

or from

$$f(x_1, x_2) = F(F_1, F_2) f_1 f_2,$$

where the two PDFs f_1 and f_2 can then be formulated from equation (2).

2.2. The BPTL-BR $\mathcal{X}\mathcal{I}\mathcal{I}$ via modified FGM model

The modified version of the FGM model can then be derived as

$$F_\rho(\hbar, \varpi) = \hbar \varpi [\rho \Phi(\hbar) \vartheta(\varpi) + 1] |_{\rho \in (-1, 1)}$$

or

$$F_\rho(\hbar, \varpi) = \hbar \varpi + \rho \tilde{\Phi}_\hbar \tilde{\vartheta}_\varpi |_{\rho \in (-1, 1)},$$

where

$$\tilde{\Phi}_\hbar = \hbar \Phi(\hbar) \text{ and } \tilde{\vartheta}_\varpi = \varpi \vartheta(\varpi).$$

The $\Phi(\hbar)$ and $\vartheta(\varpi)$ are two functions continuous on $(0, 1)$ where

$$\Phi(0) = \Phi(1) = \vartheta(0) = \vartheta(1) = 0.$$

Let

$$\begin{aligned} d_1 &= d_1(\tilde{\Phi}_\hbar) = \inf \left\{ \tilde{\Phi}_\hbar : \frac{\partial}{\partial \hbar} \tilde{\Phi}_\hbar |_{\sigma_1} \right\} < 0, \\ d_2 &= d_2(\tilde{\Phi}_\hbar) = \sup \left\{ \tilde{\Phi}_\hbar : \frac{\partial}{\partial \hbar} \tilde{\Phi}_\hbar |_{\sigma_1} \right\} < 0, \end{aligned}$$

$$\begin{aligned} e_1 &= e_1(\tilde{\vartheta}_\varpi) = \inf \left\{ \tilde{\vartheta}_\varpi : \frac{\partial}{\partial \varpi} \tilde{\vartheta}_\varpi |_{\sigma_2} \right\} > 0, \\ e_2 &= e_2(\tilde{\vartheta}_\varpi) = \sup \left\{ \tilde{\vartheta}_\varpi : \frac{\partial}{\partial \varpi} \tilde{\vartheta}_\varpi |_{\sigma_2} \right\} > 0. \end{aligned}$$

Then,

$$1 \leq \min(d_1 d_2, e_1 e_2) < \infty,$$

where

$$\begin{aligned} \hbar \frac{\partial}{\partial \hbar} \Phi(\hbar) &= \frac{\partial}{\partial \hbar} \tilde{\Phi}_\hbar - \Phi(\hbar), \\ \sigma_1 &= \left\{ \hbar : \hbar \in (0, 1) \mid \frac{\partial}{\partial \hbar} \tilde{\Phi}_\hbar \text{ exists} \right\} \end{aligned}$$

and

$$\sigma_2 = \left\{ \varpi : \varpi \in (0, 1) \mid \frac{\partial}{\partial \varpi} \tilde{\vartheta}_\varpi \text{ exists} \right\}.$$

2.2.1. Type-I BPTL-BR $\mathcal{X}\mathcal{I}\mathcal{I}$ -FGM version For deriving the type-I BPTL-BR $\mathcal{X}\mathcal{I}\mathcal{I}$ -FGM model, we consider the two continuous functional forms $\Phi(\hbar)$ and $\vartheta(\varpi)$.

Then, the type-I BPTL-BR $\mathcal{X}\mathcal{I}\mathcal{I}$ -FGM can be written from

$$F_\rho(\hbar, \varpi)|_{\rho \in (-1, 1)} = \hbar\varpi + \rho\tilde{\Phi}_\hbar\tilde{\vartheta}_\varpi$$

where

$$\tilde{\Phi}_\hbar = \hbar\overline{F_{\underline{\psi}_1}(\hbar)}|_{\overline{F_{\underline{\psi}_1}(\hbar)}} = [1 - F_{\underline{\psi}_1}(\hbar)],$$

and

$$\tilde{\vartheta}_\varpi = \varpi\overline{F_{\underline{\psi}_2}(\varpi)}|_{\overline{F_{\underline{\psi}_2}(\varpi)}} = [1 - F_{\underline{\psi}_2}(\varpi)].$$

Then, the type-I BPTL-BR $\mathcal{X}\mathcal{I}\mathcal{I}$ -FGM can then directly be written as

$$\begin{aligned} F_\rho(\hbar, \varpi)|_{\rho \in (-1, 1)} &= \varkappa_{[\theta_1]}^{-1} \left(1 - \exp \left\{ -\theta_1 [\xi_{\theta_2}(\hbar)^{-2\beta_2}]^{\beta_1} \right\} \right) \\ &\quad \times \varkappa_{[c_1]}^{-1} \left(1 - \exp \left\{ -c_1 [\xi_{c_2}(\varpi)^{-2b_2}]^{b_1} \right\} \right) \\ &\quad + \rho\tilde{\Phi}_\hbar\tilde{\vartheta}_\varpi, \end{aligned}$$

where

$$\begin{aligned} \tilde{\Phi}_\hbar &= \varkappa_{[\theta_1]}^{-1} \left(1 - \exp \left\{ -\theta_1 [\xi_{\theta_2}(\hbar)^{-2\beta_2}]^{\beta_1} \right\} \right) \\ &\quad \times \left[1 - \varkappa_{[\theta_1]}^{-1} \left(1 - \exp \left\{ -\theta_1 [\xi_{\theta_2}(\hbar)^{-2\beta_2}]^{\beta_1} \right\} \right) \right], \end{aligned}$$

and

$$\begin{aligned} \tilde{\vartheta}_\varpi &= \varkappa_{[c_1]}^{-1} \left(1 - \exp \left\{ -c_1 [\xi_{c_2}(\varpi)^{-2b_2}]^{b_1} \right\} \right) \\ &\quad \times \left[1 - \varkappa_{[c_1]}^{-1} \left(1 - \exp \left\{ -c_1 [\xi_{c_2}(\varpi)^{-2b_2}]^{b_1} \right\} \right) \right] \end{aligned}$$

2.2.2. Type-II BPTL-BR $\mathcal{X}\mathcal{I}\mathcal{I}$ -FGM model For deriving the type-II BPTL-BR $\mathcal{X}\mathcal{I}\mathcal{I}$ -FGM model, let $\Phi(\hbar)^*$ and $\vartheta(\varpi)^*$ be two functional forms where

$$\Phi(\hbar)^*|_{(\rho_1 > 0)} = \hbar^{\rho_1} (1 - \hbar)^{1-\rho_1}$$

and

$$\vartheta(\varpi)^*|_{(\rho_2 > 0)} = \varpi^{\rho_2} (1 - \varpi)^{1-\rho_2}.$$

Then, the type-II BPTL-BR $\mathcal{X}\mathcal{I}\mathcal{I}$ -FGM obtained from

$$F_{\rho, \rho_1, \rho_2}(\hbar, \varpi)|_{(\rho_1 > 0)} = \mu\nu [1 + \rho\Phi(\hbar)^* \vartheta(\varpi)^*].$$

Then, the type-II BPTL-BR $\mathcal{X}\mathcal{I}\mathcal{I}$ -FGM can be written as

$$\begin{aligned} F_{\rho, \rho_1, \rho_2}(\hbar, \varpi)|_{(\rho_1 > 0)} &= \varkappa_{[\theta_1]}^{-1} \left(1 - \exp \left\{ -\theta_1 [\xi_{\theta_2}(\hbar)^{-2\beta_2}]^{\beta_1} \right\} \right) \\ &\quad \times \left[1 - \varkappa_{[c_1]}^{-1} \left(1 - \exp \left\{ -c_1 [\xi_{c_2}(\varpi)^{-2b_2}]^{b_1} \right\} \right) \right] \\ &\quad \times [1 + \rho\Phi(\hbar)^* \vartheta(\varpi)^*], \end{aligned}$$

where

$$\begin{aligned}\Phi(\hbar)^* &= \left[\varkappa_{[\theta_1]}^{-1} \left(1 - \exp \left\{ -\theta_1 [\xi_{\theta_2}(\hbar)^{-2\beta_2}]^{\beta_1} \right\} \right) \right]^{\rho_1} \\ &\quad \times \left[1 - \varkappa_{[\theta_1]}^{-1} \left(1 - \exp \left\{ -\theta_1 [\xi_{\theta_2}(\hbar)^{-2\beta_2}]^{\beta_1} \right\} \right) \right]^{1-\rho_1},\end{aligned}$$

and

$$\begin{aligned}\vartheta(\varpi)^* &= \left[\varkappa_{[c_1]}^{-1} \left(1 - \exp \left\{ -c_1 [\xi_{c_2}(\varpi)^{-2b_2}]^{b_1} \right\} \right) \right]^{\rho_2} \\ &\quad \times \left[1 - \varkappa_{[c_1]}^{-1} \left(1 - \exp \left\{ -c_1 [\xi_{c_2}(\varpi)^{-2b_2}]^{b_1} \right\} \right) \right]^{1-\rho_2}.\end{aligned}$$

2.2.3. Type-III BPTL-BR \mathcal{XII} -FGM model For deriving the type-II BPTL-BR \mathcal{XII} -FGM model, let

$$\widetilde{\Phi^*(\hbar)} = \hbar [\log(\hbar^* + 1)]$$

and

$$\widetilde{\vartheta^*(\varpi)} = \varpi [\log(\varpi^* + 1)]$$

for all $\widetilde{\Phi^*(\hbar)}$ and $\widetilde{\vartheta^*(\varpi)}$. In this case, the CDF of the type-III BPTL-BR \mathcal{XII} -FGM can then be obtained from

$$F_\rho(\hbar, \varpi) = \hbar \varpi \left(1 + \rho \widetilde{\Phi^*(\hbar)} \widetilde{\vartheta^*(\varpi)} \right),$$

and can be written as

$$\begin{aligned}F_\rho(\hbar, \varpi) &= \varkappa_{[\theta_1]}^{-1} \left(1 - \exp \left\{ -\theta_1 [\xi_{\theta_2}(\hbar)^{-2\beta_2}]^{\beta_1} \right\} \right) \\ &\quad \times \varkappa_{[c_1]}^{-1} \left(1 - \exp \left\{ -c_1 [\xi_{c_2}(\varpi)^{-2b_2}]^{b_1} \right\} \right) \\ &\quad \times \left(1 + \rho \widetilde{\Phi^*(\hbar)} \widetilde{\vartheta^*(\varpi)} \right),\end{aligned}$$

where

$$\begin{aligned}\widetilde{\Phi^*(\hbar)} &= \varkappa_{[\theta_1]}^{-1} \left(1 - \exp \left\{ -\theta_1 [\xi_{\theta_2}(\hbar)^{-2\beta_2}]^{\beta_1} \right\} \right) \\ &\quad \times \log \left[2 - \varkappa_{[c_1]}^{-1} \left(1 - \exp \left\{ -c_1 [\xi_{c_2}(\varpi)^{-2b_2}]^{b_1} \right\} \right) \right],\end{aligned}$$

and

$$\begin{aligned}\widetilde{\vartheta^*(\varpi)} &= \varkappa_{[c_1]}^{-1} \left(1 - \exp \left\{ -c_1 [\xi_{c_2}(\varpi)^{-2b_2}]^{b_1} \right\} \right) \\ &\quad \times \log \left[2 - \varkappa_{[\theta_1]}^{-1} \left(1 - \exp \left\{ -\theta_1 [\xi_{\theta_2}(\hbar)^{-2\beta_2}]^{\beta_1} \right\} \right) \right].\end{aligned}$$

2.3. The BPTL-BR \mathcal{XII} via the copula of Clayton

The copula of Clayton can be considered as

$$F(\varpi_1, \varpi_2) = [(1/\varpi_1)^\rho - 1 + (1/\varpi_2)^\rho]^{-\rho^{-1}}|_{\rho \in (0, \infty)}.$$

Then, setting $\varpi_1 = F_{\underline{\psi}_1}(t)$ and $\varpi_2 = F_{\underline{\psi}_2}(x)$ where

$$\varpi_1 = F_{\underline{\psi}_1}(t) = \varkappa_{[\theta_1]}^{-1} \left(1 - \exp \left\{ -\theta_1 [\xi_{\theta_2}(\varpi_1)^{-2\beta_2}]^{\beta_1} \right\} \right)$$

and

$$\varpi_2 = F_{\underline{\psi}_2}(x) = \varkappa_{[c_1]}^{-1} \left(1 - \exp \left\{ -c_1 [\xi_{c_2}(\varpi_2)^{-2b_2}]^{b_1} \right\} \right).$$

Then, the BPTL-BR $\mathcal{X}\mathcal{I}\mathcal{I}$ type under the Clayton copula can be derived from

$$F(\varpi_1, \varpi_2) = \left\{ \begin{array}{l} \left[\frac{1}{\varkappa_{[\theta_1]}^{-1}(1-\exp\{-\theta_1[\xi_{\theta_2}(\varpi_1)^{-2\beta_2}]^{\beta_1}\})} \right]^\rho \\ + \left[\frac{1}{\varkappa_{[c_1]}^{-1}(1-\exp\{-c_1[\xi_{c_2}(\varpi_2)^{-2b_2}]^{b_1}\})} \right]^\rho - 1 \end{array} \right\}^{-\rho^{-1}} \Big|_{\rho \in (0, \infty)}.$$

Similarly and using the same statistical copula technique, the MPTL-BR $\mathcal{X}\mathcal{I}\mathcal{I}$ can be then derived.

2.4. The BPTL-BR $\mathcal{X}\mathcal{I}\mathcal{I}$ via Renyi Copula

Using the theorem of Pougaza and Djafari [34] for getting the BPTL-BR $\mathcal{X}\mathcal{I}\mathcal{I}$ via Renyi copula, we have

$$F(x_1, x_2) = x_2 \hbar + x_1 \varpi - x_1 x_2.$$

Then, the associated BPTL-BR $\mathcal{X}\mathcal{I}\mathcal{I}$ via Renyi copula will be

$$\begin{aligned} F(\hbar, \varpi) &= x_2 \varkappa_{[\theta_1]}^{-1} \left(1 - \exp \left\{ -\theta_1 [\xi_{\theta_2}(x_1)^{-2\beta_2}]^{\beta_1} \right\} \right) \\ &\quad + x_1 \varkappa_{[c_1]}^{-1} \left(1 - \exp \left\{ -c_1 [\xi_{c_2}(x_2)^{-2b_2}]^{b_1} \right\} \right) \\ &\quad - x_1 x_2. \end{aligned}$$

3. Applications under uncensored samples

In this part, we provide and analyze four complete real-life data for applications to four real datasets for illustrating the importance and the wide potentiality of the PTL-BR $\mathcal{X}\mathcal{I}\mathcal{I}$ model. dataset I (given and reported by Nichols & Padgett [40]) can be called the monotonically increasing failure stress data (or breaking of stress data) which consists of 100 observations. dataset II is called the monotonically increasing failure survival times (or the survival data) in days of 72 of the pigs of Guinea which are infected with the virulent tubercle bacilli, these real-life dataset (see Bjerkedal [11]). dataset III can be called as the monotonically increasing failure revenue of taxes data (or the economic data) in the Egyptian pounds. dataset IV (the leukaemia dataset) is called the U-failure leukaemia data where this real-life dataset gives the survival times of 33 patients whom suffering from the well-known acute leukaemia (myelogenous). The four datasets are given in the literature. More useful real data are available in Shehata et al., [47] and Shehata and Yousof ([44], [45], [46]).

For weighting and in order to compare the fitted models under those real datasets, we consider the following goodness-of-fit statistics for the uncensored samples:

- The Akaike Information criterion (ICr) $T_{(AI)}$;
- The coordinated (consistent) Akaike ICr $T_{(CAI)}$.

- The Quinn and Hannan ICr $T_{(HQI)}$;
- The Bayesian ICr $T_{(BI)}$;

Table 1: MaxLEs, St.Ers and CIs results for the dataset I.

Competition Models	$\widehat{\theta}_1, \widehat{\beta}_1, \widehat{\theta}_2, \widehat{\beta}_2, \widehat{\gamma}$
BR \mathcal{X}^{II}	—, —, 5.941, 0.1873, — —, —, (1.2794), (0.0443), — —, —, (3.43,8.454), (0.10,0.272), —
MO-BR \mathcal{X}^{II}	—, —, 1.19231, 4.83456, 838.7343 —, —, (0.9522), (4.8960), (229.344) —, —, (0, 3.068), (0, 14.435), (389.20,1288.247)
TL-BR \mathcal{X}^{II}	—, —, 1.3502, 1.0613, 13.7283 —, —, (0.3783), (0.3842), (8.401) —, —, (0.61, 2.092), (0.31,1.821), (0, 30.194)
KUM-BR \mathcal{X}^{II}	48.1032, 79.5166, 0.3511, 2.7301, — (19.35), (58.1867), (0.1), (1.08), — (10.18,86.1), (0,193.562), (0.16,0.544), (0.62,4.844), —
B-BR \mathcal{X}^{II}	359.6833, 260.1, 0.1755, 1.1233, — (57.9432), (132.214), (0.0133), (0.2433), — (246.12,473.3), (0.962,519), (0.14,0.203), (0.651,1.6), —
BE-BR \mathcal{X}^{II}	0.381, 11.949, 0.937, 33.402, 1.705 (0.078), (4.635), (0.267), (6.287),(0.478) (0.2,0.5), (2.7,21), (0.4,1.5), (21.1,45.7), (0.8,2.6)
FB-BR \mathcal{X}^{II}	0.42134, 0.8344, 6.112, 1.6744, 3.4503 (0.01), (0.9), (2.3), (0.23), (1.96) (0.33,0.4), (0, 2.68), (1.57, 10.65), (1.23, 2.12), (0, 7.29)
FKUM-BR \mathcal{X}^{II}	0.5424, 4.22345, 5.31353, 0.4112, 4.1525 (0.1372), (1.8822), (2.3180), (0.4971), (1.9950) (0.25, 0.84), (0.5,7.95), (0.77,9.89), (0, 1.37), (0.24,8.1)
ZgB-BR \mathcal{X}^{II}	123.1013, —, 0.3684, 139.2476, — (243.0113), —, (0.34324), (318.5463), — (0, 599.42), —,(0, 1.044), (0, 763.592), —
PTL-BR \mathcal{X}^{II}	—185.4643, 0.01745, 3, 0.2923, — (295.23), (0.0258), (0.645), (0.0921), — (-763.7,382.7), (-0.03,0.68), (1.7,4.26), (0.12,0.47), —

Table 1 gives and lists the estimates of the maximum likelihood (MaxLEs), the corresponding standard errors (St.Ers), 99% confidence intervals (99%CIs) for the dataset I. Table 2 gives the MaxLEs, St.Ers and 99%CIs results for the dataset II. Table 3 gives the MaxLEs, St.Ers and 99%CIs results for the dataset III. Table 4 gives the MaxLEs, St.Ers and 99%CIs results for the dataset IV. Table 5 gives the $T_{(AI)}$, $T_{(BI)}$, $T_{(CAI)}$ and $T_{(HQI)}$ results for the dataset I. Table 6 gives the $T_{(AI)}$, $T_{(BI)}$, $T_{(CAI)}$ and $T_{(HQI)}$ results for the dataset II. Table 7 gives the $T_{(AI)}$, $T_{(BI)}$, $T_{(CAI)}$ and $T_{(HQI)}$ results for the dataset III. Table 8 gives the $T_{(AI)}$, $T_{(BI)}$, $T_{(CAI)}$ and $T_{(HQI)}$ results for the dataset IV. Based on the results and results in Tables 5-8 the PTL-BR \mathcal{X}^{II} model provides adequate results after comparing the novel model to the other relevant BRXII model such as the Marshall-Olkin BRXII (MOBRXII), Topp Leone BRXII (TL-BR \mathcal{X}^{II}), Zografos and Balakrishnan BRXII (ZgB-BR \mathcal{X}^{II}), 5-Parameters beta BRXII (FB-BRXII), beta BRXII, Beta exponentiated BRXII (BE-BR \mathcal{X}^{II}), 5-parameters Kumaraswamy BRXII (FKUM-BR \mathcal{X}^{II}) and Kumaraswamy BRXII (KUM-BR \mathcal{X}^{II}) models (see Yousof et al., [51], Altun et al., [9] and Altun et al., [10]). Specifically, the following results can be spotted:

- For the real-life dataset I, the PTL-BR $\mathcal{X}\mathcal{I}\mathcal{I}$ model can be strongly recommended to be the best one (version) among all other competing and relevant models with small results for $T_{(AI)}$, $T_{(BI)}$, $T_{(CAI)}$ and $T_{(HQI)}$, where $T_{(AI)} = 264.7963$, $T_{(BI)} = 275.217$, $T_{(CAI)} = 265.2174$ and $T_{(HQI)} = 269.0138$.
- For the real-life dataset II, the PTL-BR $\mathcal{X}\mathcal{I}\mathcal{I}$ model can be strongly recommended to be the best one (version) among all other competing and relevant models with small results with: $T_{(AI)} = 139.4206$, $T_{(BI)} = 148.5272$, $T_{(CAI)} = 140.0176$ and $T_{(HQI)} = 143.046$.
- For the economic dataset (dataset III), the PTL-BR $\mathcal{X}\mathcal{I}\mathcal{I}$ model can be strongly recommended to be the best one (version) among all other competing and relevant models with small results with: $T_{(AI)} = 376.37$, $T_{(BI)} = 384.68$, $T_{(CAI)} = 377.11$ and $T_{(HQI)} = 379.61$.
- For the real-life dataset IV, the PTL-BR $\mathcal{X}\mathcal{I}\mathcal{I}$ model can be strongly recommended to be the best one (version) among all other competing and relevant models with small results with: $T_{(AI)} = 295.6852$, $T_{(BI)} = 301.6712$, $T_{(CAI)} = 297.1138$ and $T_{(HQI)} = 297.6993$.

Many useful graphical tools (diagrams) are used and analyzed in this Section for more deep statistical analysis and accuracy such as the total time in test (TTT)"diagrams, the "nonparametric Kernel density estimation", the diagrams and the box diagrams, Quantile-Quantile"(Q-Q) diagrams and scattergram diagrams.

Table 2: MaxLEs, St.Ers and CIs results for the dataset II.

Competition Models	$\widehat{\theta}_1, \widehat{\beta}_1, \widehat{\theta}_2, \widehat{\beta}_2, \widehat{\gamma}$
BR $\mathcal{X}\mathcal{I}\mathcal{I}$	—, —, 3.10222, 0.46554, — —, —, (0.5381), (0.07701), — —, —, (2.044,4.2), (0.3,0.66), —
MO-BR $\mathcal{X}\mathcal{I}\mathcal{I}$	—, —, 2.25932, 1.5333, 6.76 —, —, (0.861), (0.911), (4.65) —, —, (0.566,4), (0.3,3), (0, 15.8)
TL-BR $\mathcal{X}\mathcal{I}\mathcal{I}$	—, —, 2.39334, 0.4582, 1.79666 —, —, (0.91), (0.24), (0.92) —, —, (0.6,4.2), (0, 0.95), (0.001,4)
KUM-BR $\mathcal{X}\mathcal{I}\mathcal{I}$	14.1051, 7.4245, 0.52521, 2.2738, — (10.8), (11.8), (0.3),(0.9), — (0, 35), (0.30.7), (0, 1.1), (0.3, 4.2), —
B-BR $\mathcal{X}\mathcal{I}\mathcal{I}$	2.5553, 6.0577, 1.81, 0.29, — (1.86), (10.39), (0.96),(0.5), — (0, 6.3), (0, 26.4), (0, 3.7),(0, 1.2), —
BE-BR $\mathcal{X}\mathcal{I}\mathcal{I}$	1.8765, 2.9918, 1.7801, 1.3414, 0.5726 (0.094), (1.731), (0.702), (0.816), (0.325) (1.6,2.1), (0, 6.4), (0.4, 3.3), (0, 2.9), (0, 1.2)
FB-BR $\mathcal{X}\mathcal{I}\mathcal{I}$	0.62146, 0.5493,3.8382, 1.3821, 1.6655 (0.5413), (1.0111), (2.7855), (2.3152), (0.4361) (0, 1.7), (0, 2.5), (0, 9.3), (0, 5.9), (0.82, 4.48)
FKKUM-BR $\mathcal{X}\mathcal{I}\mathcal{I}$	0.5588, 0.3087, 3.9999, 2.1315, 1.4754 (0.4422), (0.3143), (2.0821), (1.833), (0.36) (0, 1.4), (0, 0.9), (0, 3.1), (0, 5.7), (0.76, 2.2)
ZgB-BR $\mathcal{X}\mathcal{I}\mathcal{I}$	2.68123, —,1.7382, 2.1362, — (2.1801), —,(1.0249), (2.4388), — (0, 6.96), —,(0, 3.76), (0, 6.94), —
PTL-BR $\mathcal{X}\mathcal{I}\mathcal{I}$	—9.9, 0.27, 4.952536, 0.48, — (71.69), (0.0023), (1.36), (0.055), — (-150.432,130.6), (0.265,0.274), (2.2,7.6), (0.37,0.58), —

Table 3: MaxLEs, St.Ers and CIs results for the dataset III.

Competition Models	$\widehat{\theta}_1, \widehat{\beta}_1, \widehat{\theta}_2, \widehat{\beta}_2, \widehat{\gamma}$
BR $\mathcal{X}II$	—, —, 5.61544, 0.0722, — —, —, (15.04802), (0.19444), — —, —, (0, 35.2), (0, 0.4499), — —, —, 8.0174, 0.4199, 70.3599
MO-BR $\mathcal{X}II$	—, —, (22.0831), (0.3120), (63.8313) —, —, (0, 51.30), (0, 1.031), (0, 195.477)
TL-BR $\mathcal{X}II$	—, —, 91.32066, 0.01221, 141.0733 —, —, (15.0710), (0.0021), (70.0281) —, —, (61.8,120.862) (0.008, 0.021) (3.9,278)
KUM-BR $\mathcal{X}II$	18.1301, 6.8507, 10.6942, 0.0813, — (3.6892), (1.0353), (1.1666), (0.0120), — (10.89,25.4), (4.83,8.9), (8.4,12.9), (0.06,0.1), —
B-BR $\mathcal{X}II$	26.7253, 9.75666, 27.3643, 0.0201, — (9.46549), (2.7811), (12.35), (0.007), — (8.2,45.3), (4.3,15.2), (3.2,51.57), (0.006,0.03), —
BE-BR $\mathcal{X}II$	2.9244, 2.9111, 3.2701, 12.4866, 0.3714 (0.5644), (0.5488), (1.2511), (6.9383), (0.787) (1.8,4.031), (1.8,4), (0.82,5.66), (0, 26.1), (0, 1.9)
FB-BR $\mathcal{X}II$	30.4401, 0.5844, 1.0893, 5.1666, 7.8622 (91.75), (1.0644), (1.0211), (8.2688), (15.04) (0, 210.3), (0, 2.7), (0, 3.1), (0, 21.4), (0, 37.3)
FKUM-BR $\mathcal{X}II$	12.8786, 1.2255, 1.6651, 1.4111, 3.7324 (3.441), (0.13), (0.04), (0.0881), (1.1722) (6.13,19.6), (1,1.5), (1.6,1.7), (1.24,1.6), (1.4,6.03)
PTL-BR $\mathcal{X}II$	—168.88, 0.489, 3.218, 0.306 (0.000), (0.000), (1.841), (0.178) —, —, (0, 6.8), (0, 0.66)

Table 4: MaxLEs, St.Ers and CIs results for the dataset IV.

Competition Models	$\widehat{\theta}_1, \widehat{\beta}_1, \widehat{\theta}_2, \widehat{\beta}_2, \widehat{\gamma}$
BR χ^{II}	—, —, 58.7111, 0.00666, —
	—, —, (42.3822), (0.0041), —
	—, —, (0, 141.782), (0, 0.012), —
MO-BR χ^{II}	—, —, 11.8380, 0.0783, 12.2516
	—, —, (4.3688), (0.0133), (7.7701)
	—, —, (0, 141.8), (0, 0.014), (0, 27.5)
TL-BR χ^{II}	—, —, 0.2812, 1.8822, 50.2155
	—, —, (0.2888), (2.40202), (176.501)
	—, —, (0, 0.86), (0, 6.6), (0, 396.2)
KUM-BR χ^{II}	9.2014, 36.4288, 0.2422, 0.9412, —
	(10.062), (35.652), (0.1677), (1.0456), —
	(0, 28.9), (0, 106.3), (0, 0.573), (0, 2.998), —
B-BR χ^{II}	96.1044, 52.1212, 0.1043, 1.230, —
	(43.2), (33.5), (0.022), (0.33), —
	(15.4, 176.9), (0, 117.7), (0.6, 0.2), (0.59, 1.9), —
BE-BR χ^{II}	0.08777, 5.01, 1.5611, 31.271, 0.3188
	(0.08), (3.8510), (0.0123), (12.941), (0.03)
	(0, 0.3), (0, 12.7), (1.54, 2), (5.9, 56.6), (0.25, 0.4)
FB-BR χ^{II}	15.1944, 32.05, 0.3, 0.5817, 21.86
	(11.60), (9.91), (0.09), (0.07), (35.55)
	(0, 38), (12.71, 52), (0.05, 0.4), (0.45, 0.7), (0, 91.5)
FKUM-BR χ^{II}	14.7332, 15.2853, 0.293, 0.8390, 0.0344
	(12.391), (18.9), (0.22), (0.85), (0.0754)
	(0, 39), (0, 52), (0, 0.7), (0, 2.5), (0, 0.2)
ZgB-BR χ^{II}	43.9733, —, 0.1577, 44.2633, —
	(38.7877), —, (0.0822), (47.6483), —
	(0, 118), —, (0, 0.3), (0, 138), —
PTL-BR χ^{II}	—312.5, 0.0064, 2.298, 0.099, —
	(19.4), (0.244), (1.672588), (1.2), —
	(-350.5, -247.5), (0, 0.48), (0, 5.6), (0, 2.5), —

Figure 1 gives the TTT diagrams for the four real-life datasets. Figure 2 gives the nonparametric Kernel density estimation diagrams for the four real datasets. Figure 3 gives the box diagrams for the four real datasets. Figure 4 gives the Q-Q diagrams for the four real datasets. Figure 5 gives the scattergram diagrams for the four real datasets. Based on Figure 1, the TTT is monotonically increasing for datasets I, II and III and upside down for the dataset IV. Based on Figure 2, the nonparametric Kernel density estimations of the four datasets are bimodal and right skewed density for datasets I, bimodal and right skewed density with heavy tail for datasets II, III and IV. Based on Figure 3, 4 and 5, it is proved that no extreme results were spotted in dataset IV. However, datasets I, II and III have some extreme results. This is indeed a good model which can be used in mathematical and statistical modeling and analysis of the extreme value datasets. It is clear from modeling datasets I, II and III that the novel PTL-BR χ^{II} model will attract more researchers to use it and develop it. On the other hand, the PTL-BR χ^{II} model can be also recommended for mathematical, statistical modeling and analysis of the non extreme value (symmetric and asymmetric) datasets.

Figure 6 gives the fitted PDF diagrams for the four real datasets ((the top-left panel for the breaking stress real dataset), (the top-right panel for survival times data), (the bottom-left panel for the economic taxes revenue dataset) and (the bottom-right panel for acute myelogenous leukaemia dataset)). Figure 7 gives the fitted CDF diagrams for the four real datasets ((the top-left panel for breaking stress of carbon

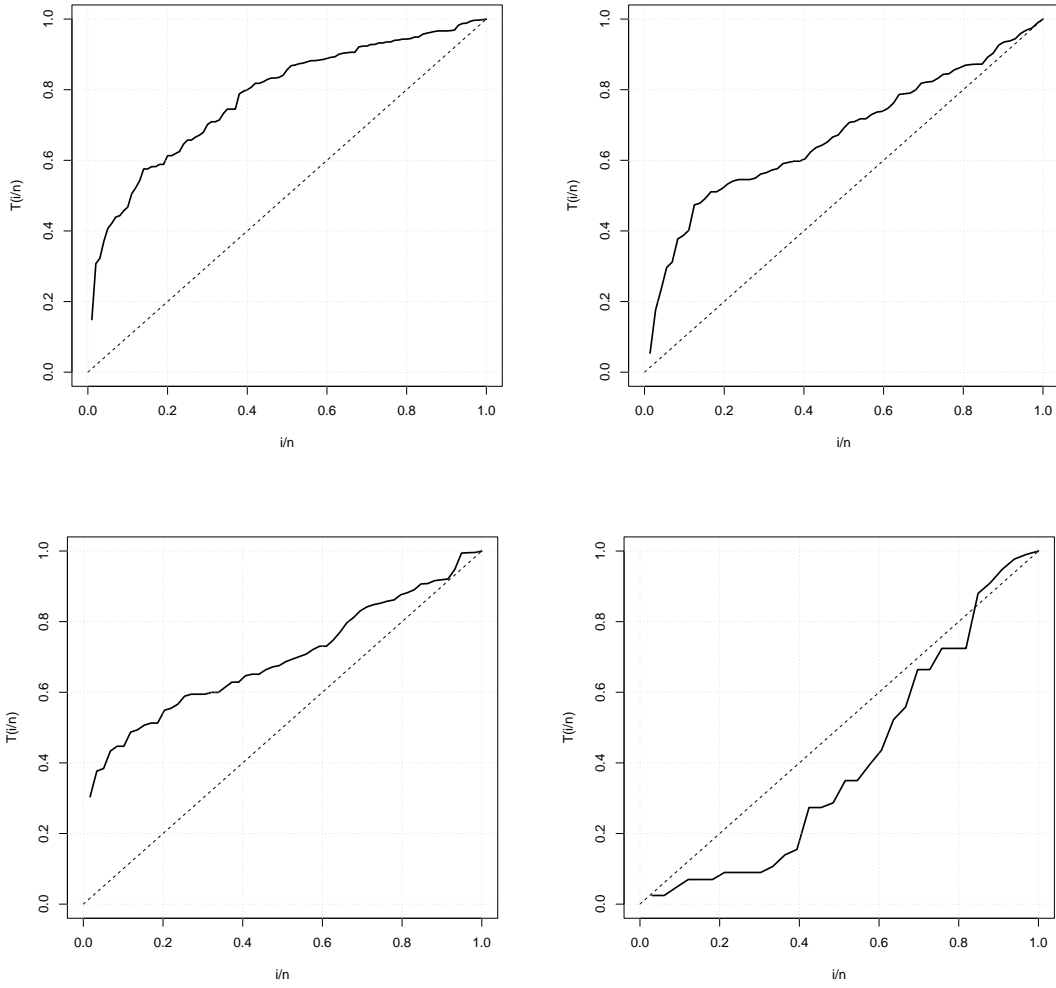


Figure 1. TTT diagrams.

fibres data), (the top-right panel for survival times data), (bottom-left panel for taxes revenue data) and (the bottom-right panel for acute myelogeneous leukaemia data)). Figure 8 gives the probability-probability (P-P) diagrams for the four real datasets ((the top-left panel for breaking stress of carbon fibres data), (the top-right panel for survival times data), (the bottom-left panel for taxes revenue data) and (the bottom-right panel for acute myelogeneous leukaemia data)). Figure 9 gives the estimated HRF diagrams for the four real datasets ((the top-left panel for breaking stress of carbon fibres data), (the top-right panel for survival times data), (the bottom-left panel for taxes revenue data) and (the bottom-right panel for acute myelogeneous leukaemia data)). Figure 10 gives the Kaplan and Meier (KM) survival diagrams for the four real datasets ((the top-left panel for breaking stress of carbon fibres data), (the top-right panel for survival times data), (the bottom-left panel for taxes revenue data) and (bottom-right panel for acute myelogeneous leukaemia data)). Based on Figure 6, Figure 7, Figure 8, Figure 9 and Figure 10, it is noted that the PTL-BR χ^2 model provides adequate fits to the four real datasets. Based on Figure 6, it is noted that the estimated HRF is upside down for all real datasets.

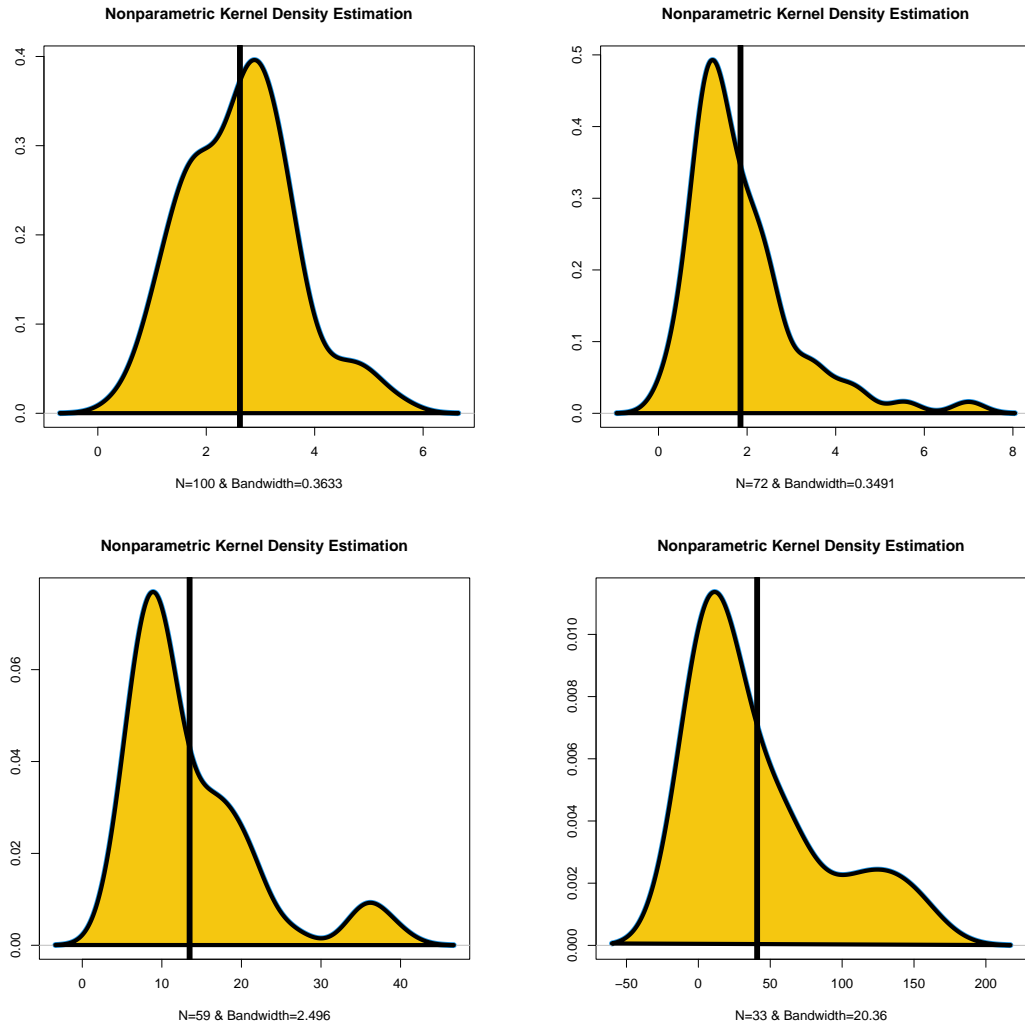


Figure 2. Kernel density estimation diagrams.

Table 5: $T_{(AI)}$, $T_{(BI)}$, $\bar{T}_{(CAI)}$ and $T_{(HQI)}$ results for the dataset I.

Competition Models	$T_{(AI)}$, $T_{(BI)}$, $\bar{T}_{(CAI)}$, $T_{(HQI)}$
BR χ^{II}	382.95, 388.16, 383.07, 385.06
MO-BR χ^{II}	305.80, 313.62, 306.10, 309.00
TL-BR χ^{II}	323.53, 331.40, 323.78, 326.71
KUM-BR χ^{II}	303.76, 314.20, 304.18, 308.00
B-BR χ^{II}	305.65, 316.10, 306.10, 309.90
BE-BR χ^{II}	305.83, 318.83, 306.47, 311.10
FB-BR χ^{II}	304.27, 317.32, 304.90, 309.57
FKUM-BR χ^{II}	305.52, 318.57, 306.17, 310.83
ZgB-BR χ^{II}	302.96, 310.78, 303.21, 306.13
PTL-BR χ^{II}	264.796, 275.21, 265.21, 269.01

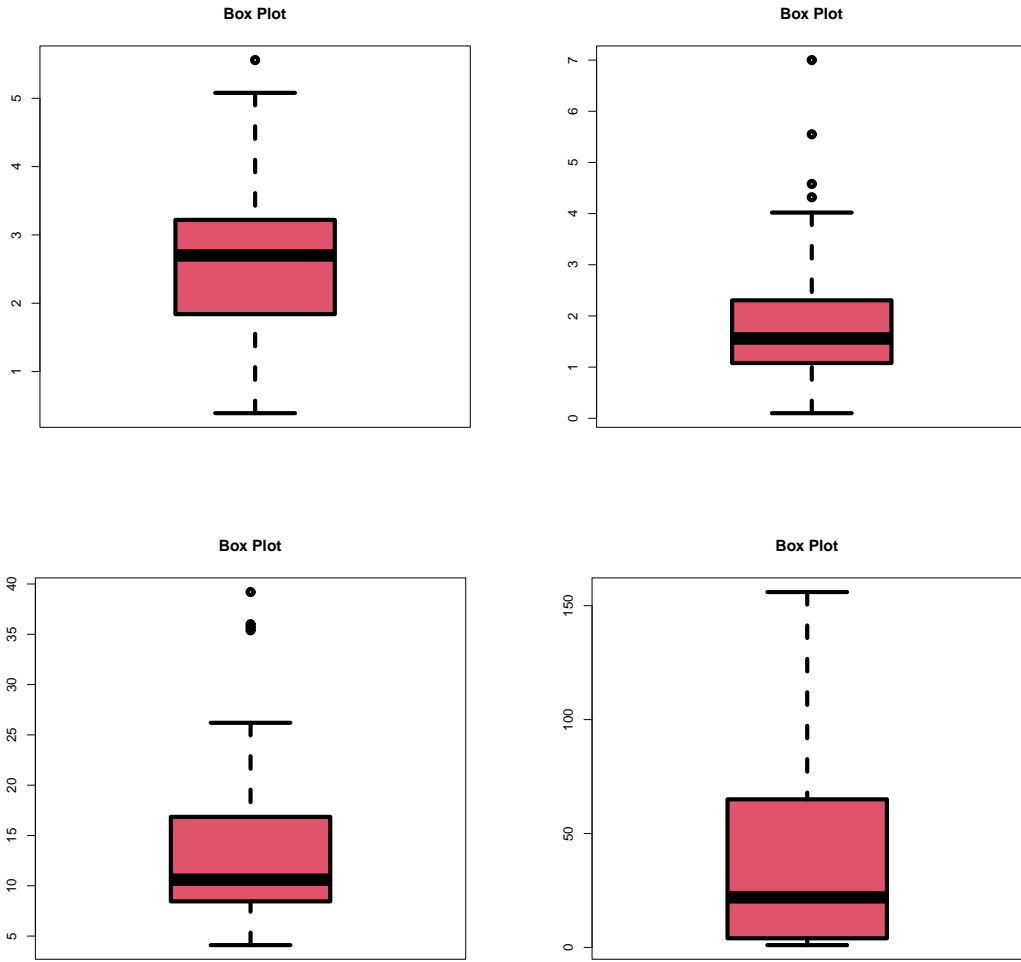


Figure 3. Box diagrams.

Table 6: $T_{(AI)}$, $T_{(BI)}$, $\bar{T}_{(CAI)}$ and $T_{(HQI)}$ results for the dataset II.

Competition Models	$T_{(AI)}$, $T_{(BI)}$, $\bar{T}_{(CAI)}$, $T_{(HQI)}$
BR $\mathcal{X}II$	209.62, 214.16, 209.78, 211.39
MO-BR $\mathcal{X}II$	209.73, 216.57, 210.10, 212.45
TL-BR $\mathcal{X}II$	211.81, 218.64, 212.16, 214.54
KUM-BR $\mathcal{X}II$	208.76, 217.86, 209.36, 212.38
B-BR $\mathcal{X}II$	210.44, 219.55, 211.05, 214.07
BE-BR $\mathcal{X}II$	212.11, 223.52, 213.01, 216.62
FB-BR $\mathcal{X}II$	206.84, 218.23, 207.73, 211.32
FKUMB- $\mathcal{X}II$	206.55, 217.93, 207.44, 211.02
ZgB-BR $\mathcal{X}II$	204.33, 211.17, 204.68, 207.05
PTL-BR $\mathcal{X}II$	139.42, 148.52, 140.01, 143.05

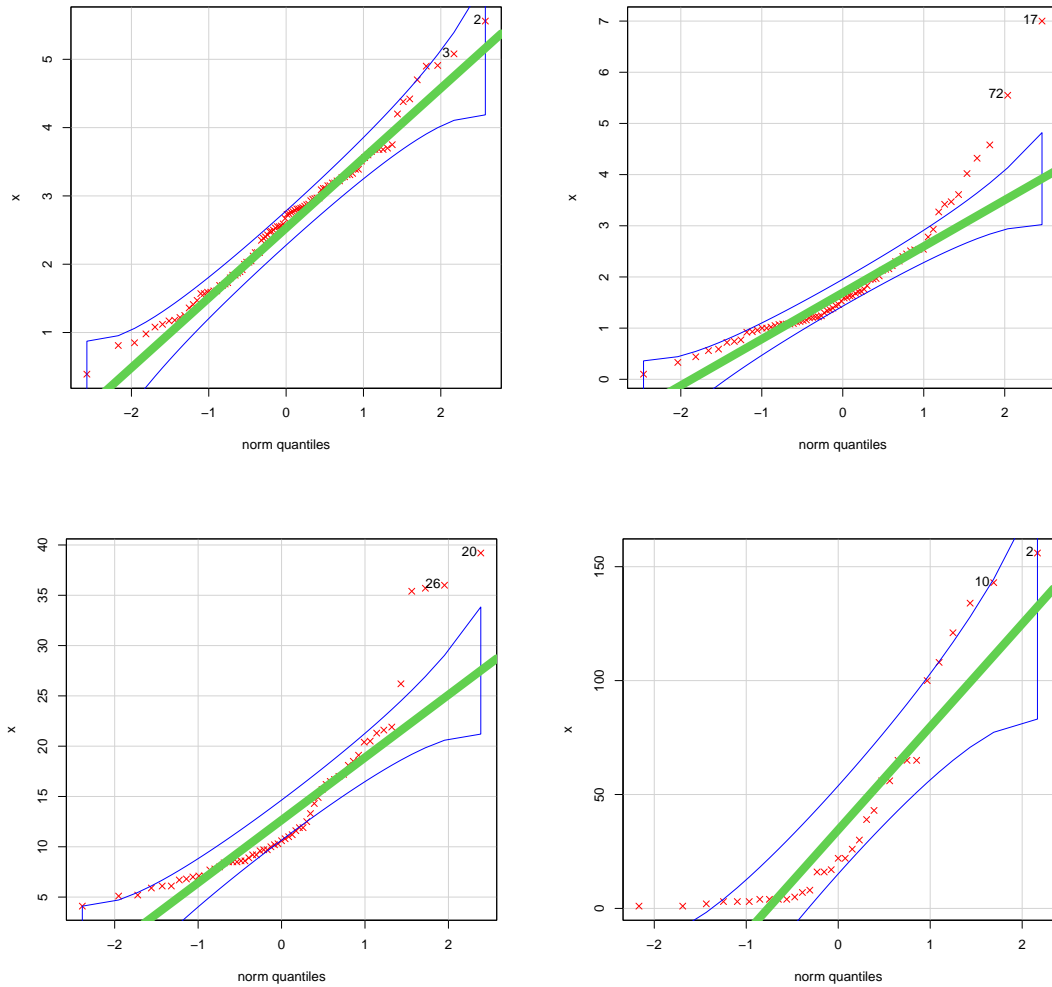


Figure 4. Q-Q diagrams.

Table 7: $T_{(AI)}$, $T_{(BI)}$, $T_{(CAI)}$ and $T_{(HQI)}$ results for the dataset III.

Competition Models	$T_{(AI)}$, $T_{(BI)}$, $T_{(CAI)}$, $T_{(HQI)}$
BR χ II	518.48, 522.60, 518.70, 520.10
MO-BR χ II	387.23, 389.40, 387.67, 389.70
TL-BR χ II	385.95, 392.20, 386.40, 388.41
KUM-BR χ II	385.60, 393.92, 386.33, 388.87
B-BR χ II	385.57, 394.11, 386.31, 389.12
BE-BR χ II	387.10, 397.43, 388.20, 391.10
FB-BR χ II	386.75, 397.15, 387.88, 390.85
FKUM-BR χ II	386.97, 397.35, 388.10, 391.10
PTL-BR χ II	376.37, 384.68, 377.11, 379.61

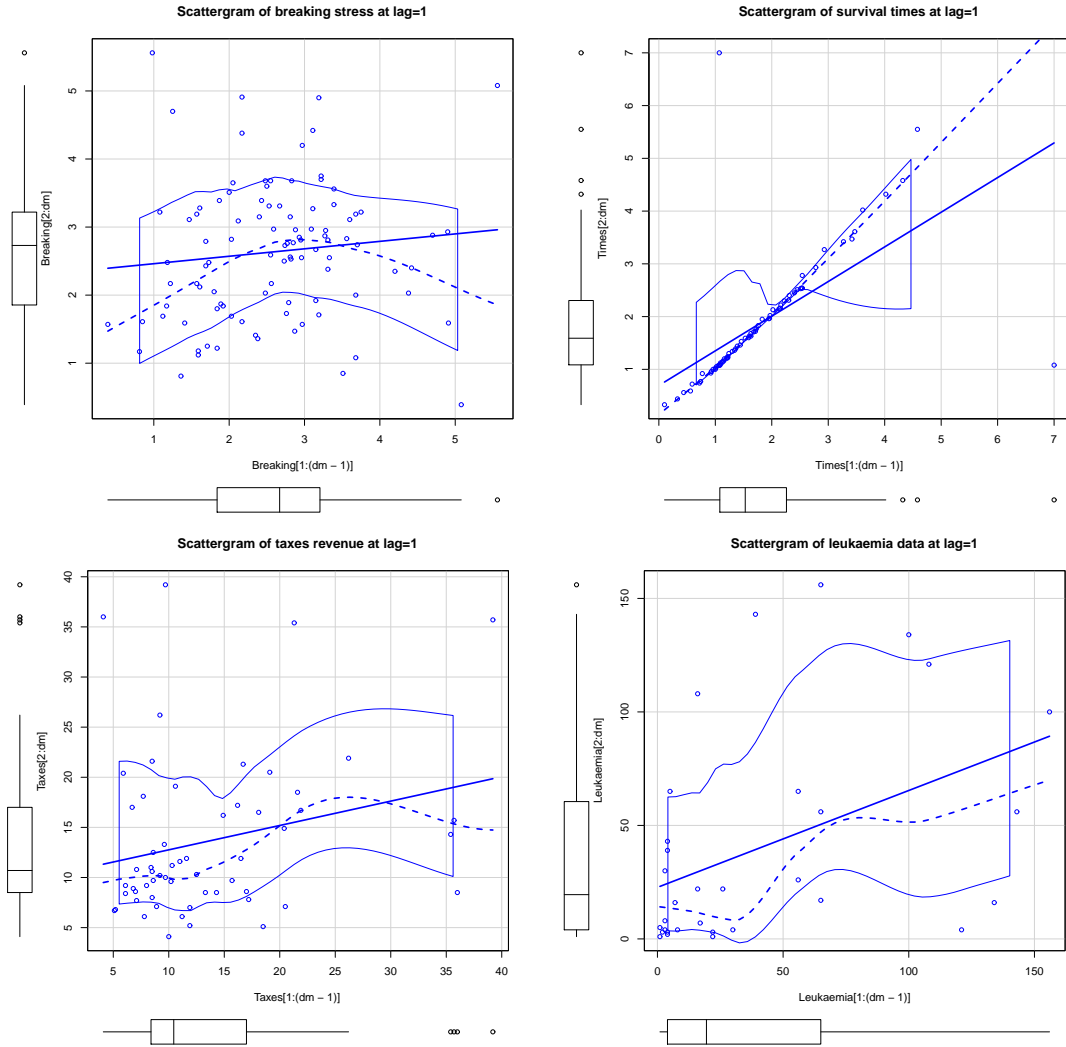


Figure 5. Scattergram plots.

Table 8: $T_{(AI)}$, $T_{(BI)}$, $T_{(CAI)}$ and $T_{(HQI)}$ results for the dataset IV.

Competition Models	$T_{(AI)}$, $T_{(BI)}$, $T_{(CAI)}$, $T_{(HQI)}$
BR χ II	328.21, 331.20, 328.62, 329.20
MO-BR χ II	315.55, 320.10, 316.40, 317.10
TL-BR χ II	316.30, 320.72, 317.10, 317.80
KUM-BR χ II	317.38, 323.33, 318.80, 319.33
B-BR χ II	316.70, 322.50, 317.90, 318.46
BE-BR χ II	317.60, 325.10, 319.82, 320.10
FB-BR χ II	317.88, 325.35, 320.10, 320.40
FKUM-BR χ II	317.70, 325.22, 319.97, 320.30
ZgB-BR χ II	313.87, 318.36, 314.40, 315.40
PTL-BR χ II	295.68, 301.67, 297.12, 297.69

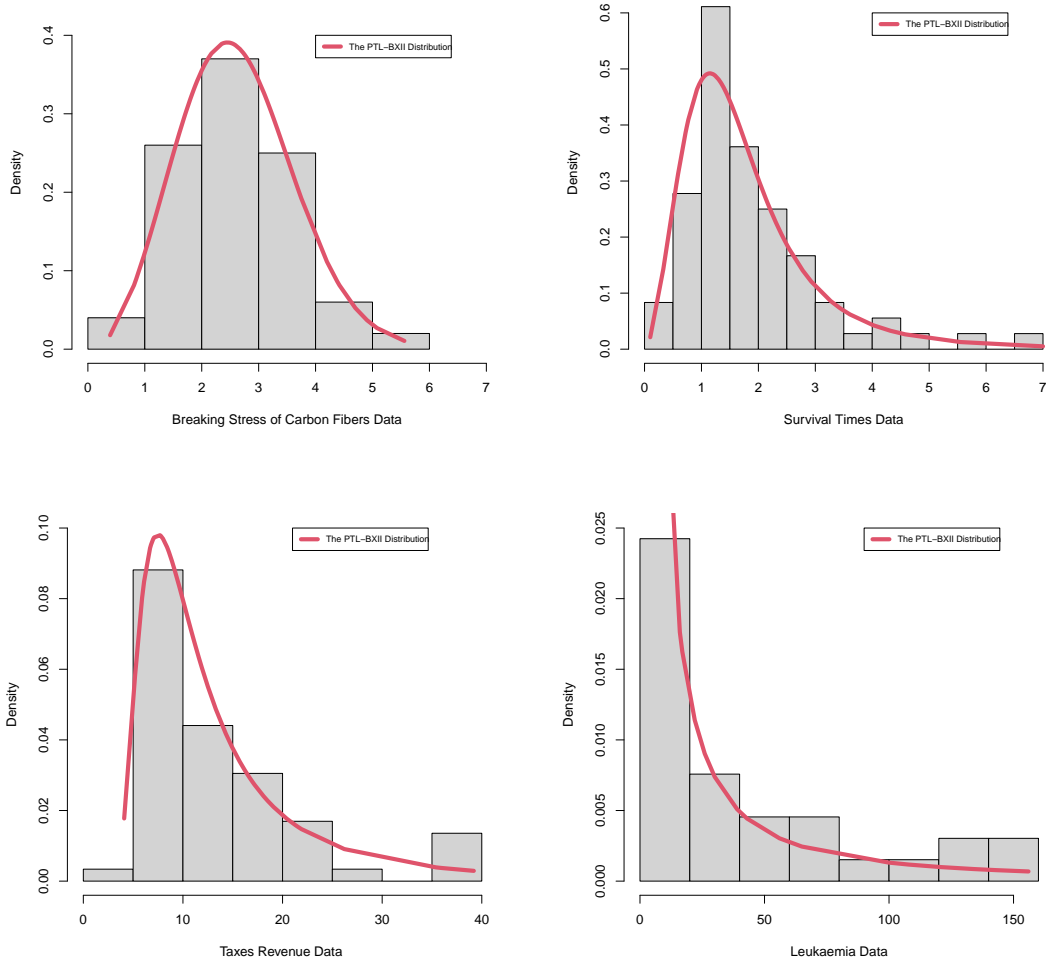


Figure 6. The fitted PDF plots.

4. Conclusions

In this article, the flexible Poisson-Topp-Leone Burr type- $\mathcal{X}\mathcal{I}\mathcal{I}$ distribution is studied and applied using some real-life datasets. For this applicable purpose, four uncensored real-life datasets are analyzed and modeled. For the uncensored samples, the Poisson-Topp-Leone Burr $\mathcal{X}\mathcal{I}\mathcal{I}$ distribution is compared with the other Burr distributions and provided the best fits under some criterion. Based on the analysis of the uncensored real datasets, it is noted that the Poisson Topp Leone Burr $\mathcal{X}\mathcal{I}\mathcal{I}$ distribution can model the uncensored engineering, economic and medical real datasets. For the bivariate modeling of the bivariate uncensored engineering and medical real-life datasets, we presented many bivariate version with some useful theoretical results. For modeling the bivariate uncensored engineering and medical real-life datasets, we presented some bivariate versions with some useful theoretical results. Those version are investigated due to certain and common copulas. Those bivariate versions are derived due to the Farlie,

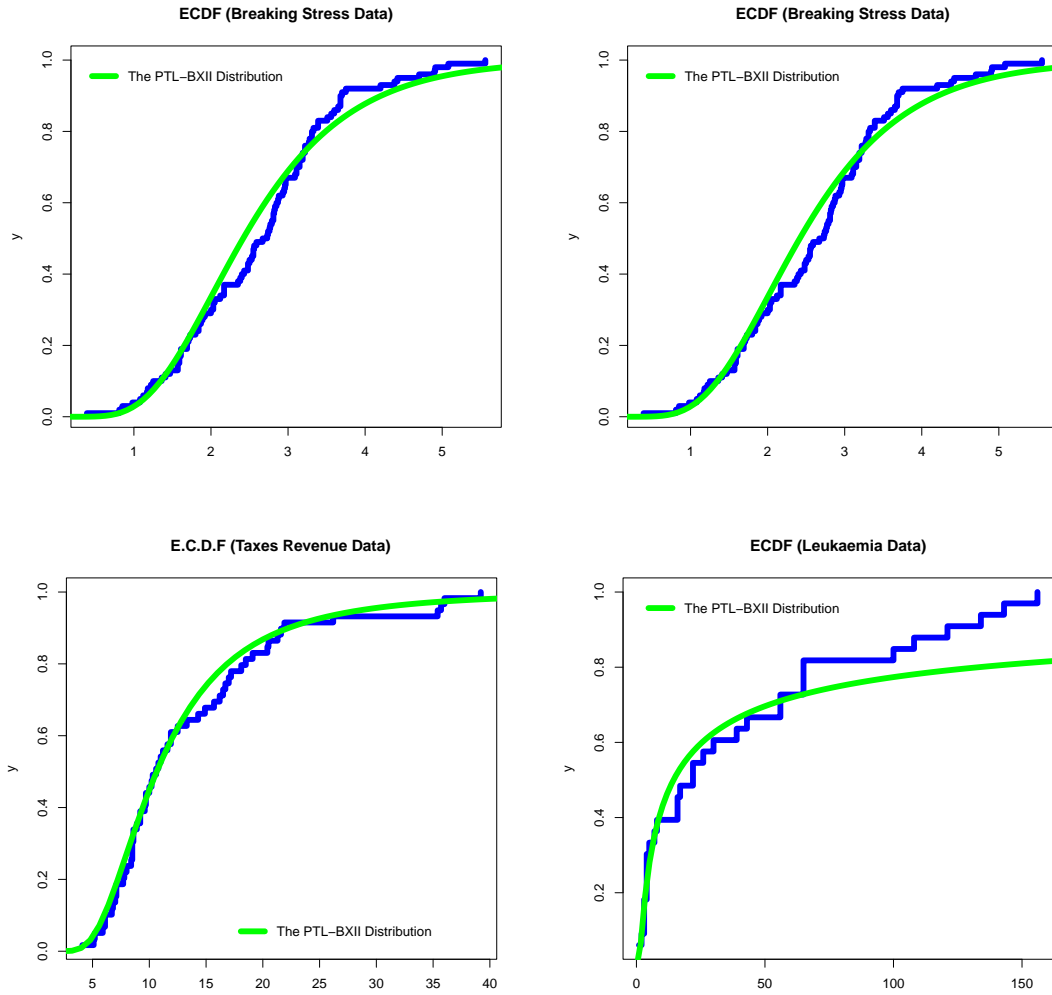


Figure 7. The fitted CDF plots.

Gumbel and Morgenstern, the entropy copula, copula of Clayton and the modified version Farlie, Gumbel and Morgenstern family.

For the extreme results datasets, and it is noted the Poisson-Topp-Leone Burr $\mathcal{X}\mathcal{I}\mathcal{I}$ distributiona is good model which can used in mathematical and statistical modeling and analysis of the extreme value datasets, the novel Poisson-Topp-Leone Burr $\mathcal{X}\mathcal{I}\mathcal{I}$ model will attract more reaserchers to use it and develope it. On the other hand, the Poisson-Topp-Leone Burr $\mathcal{X}\mathcal{I}\mathcal{I}$ model can be also recommended for mathematical, statistical modeling and analysis of the non extreme value (symmetric and asymmetric) datasets. The Poisson-Topp-Leone Burr $\mathcal{X}\mathcal{I}\mathcal{I}$ model can be also recommended for mathematical, statistical modeling and analysis of the monotonically increasing failure rate and U-failure rate datasets. For the bivariate (symmetric and asymmetric) datasets, the Poisson-Topp-Leone Burr $\mathcal{X}\mathcal{I}\mathcal{I}$ model can be also recommended either it was left skewed (symmetric and asymmetric) datasets or right skewed (symmetric and asymmetric) datasets.

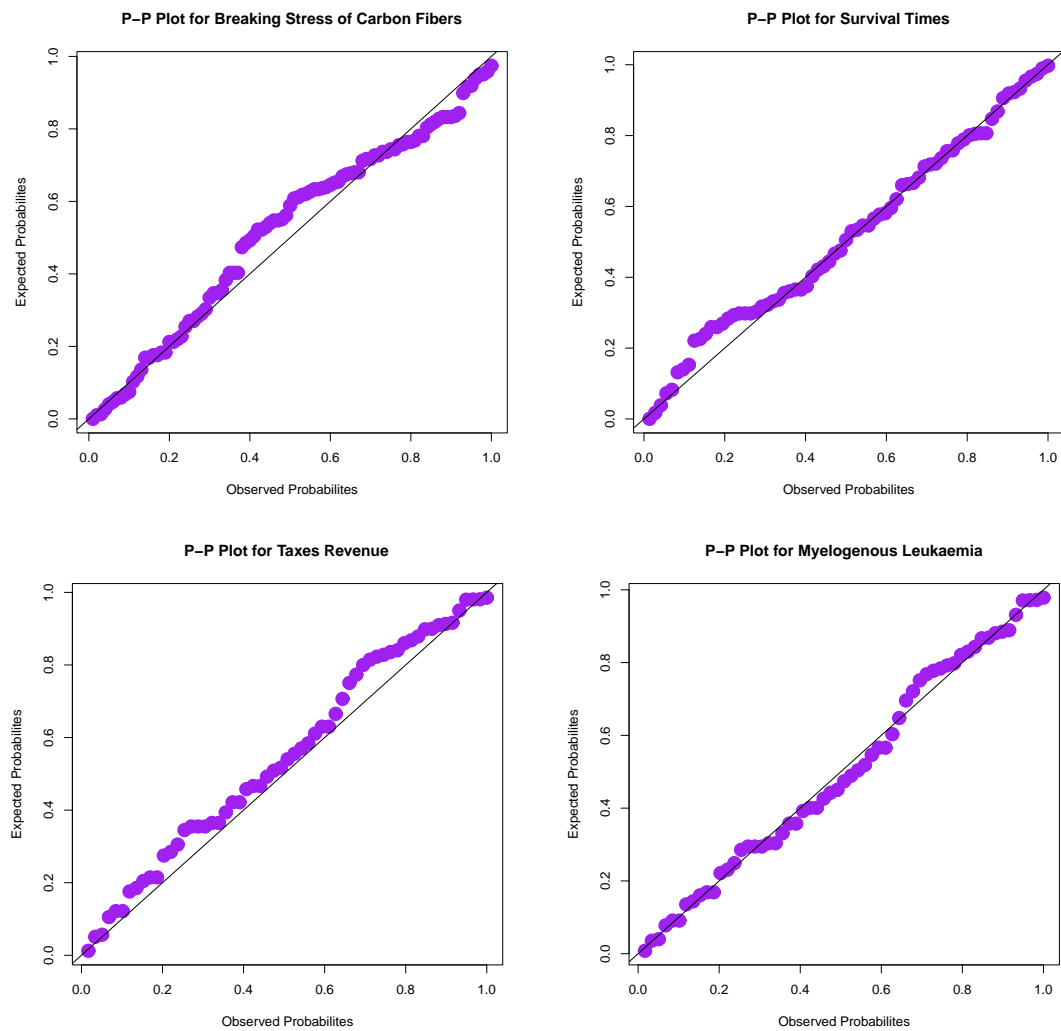


Figure 8. The P-P plots.

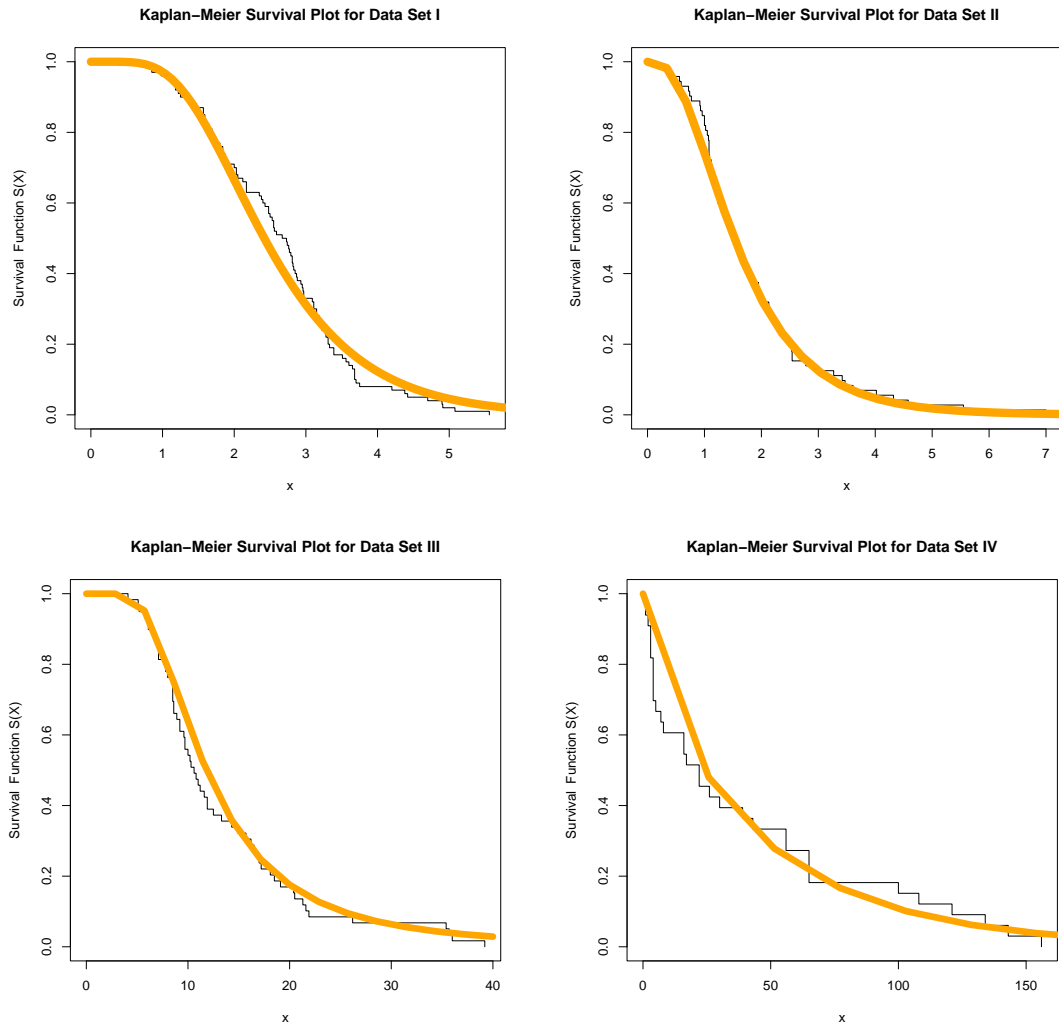


Figure 9. The KM plots.

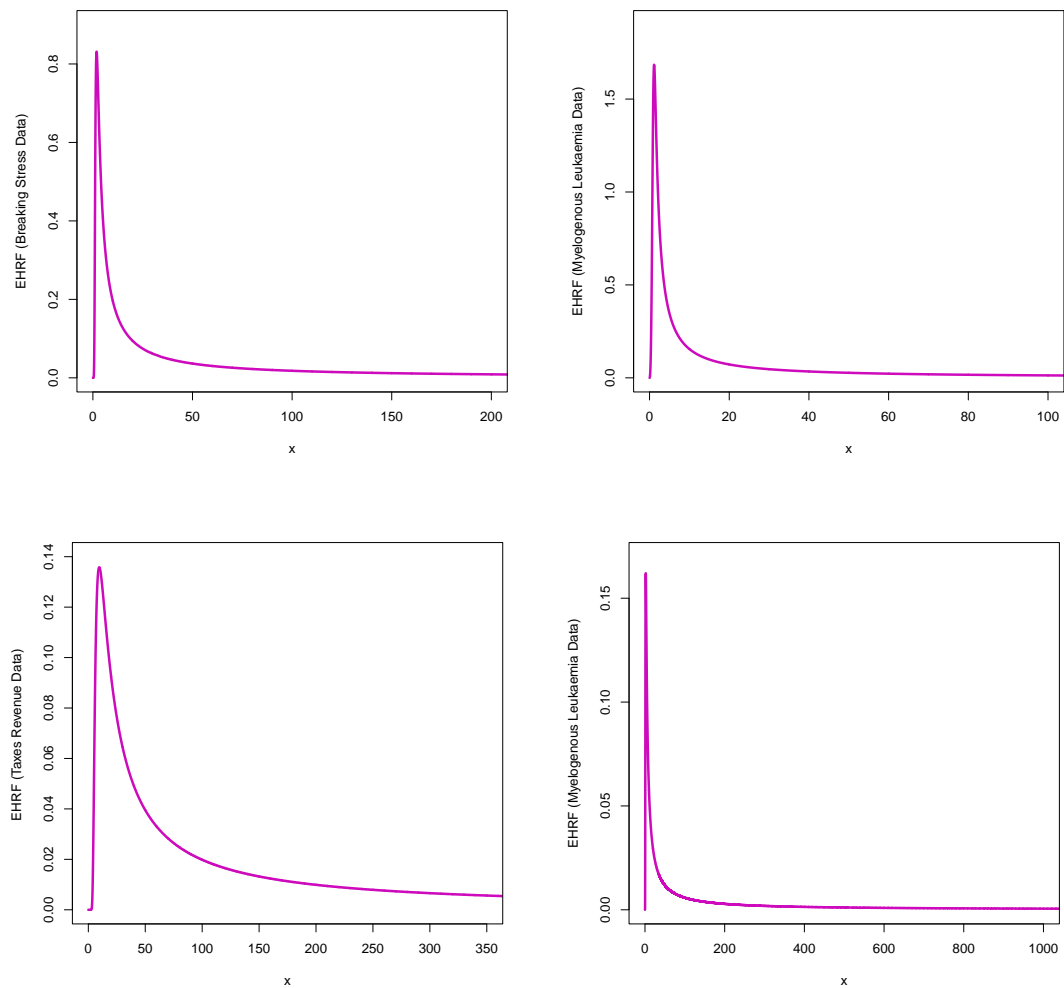


Figure 10. The EHRF plots.

REFERENCES

1. Abouelmagd, T. H. M., Hamed, M. S., Hamedani, G. G., Ali, M. M., Goual, H., Korkmaz, M. C., & Yousof, H. M. (2019a). The zero truncated Poisson Burr X family of distributions with properties, characterizations, applications, and validation test. *Journal of Nonlinear Sciences and Applications*, 12(5), 314-336.
2. Abouelmagd, T. H. M., Hamed, M. S., Handique, L., Goual, H., Ali, M. M., Yousof, H. M., & Korkmaz, M. C. (2019b). A new class of distributions based on the zero truncated Poisson distribution with properties and applications. *Journal of Nonlinear Sciences & Applications (JNSA)*, 12(3), 152-164.
3. Ali, M. M., Ali, I., Yousof, H. M. and Ibrahim, M. (2022). G Families of Probability Distributions: Theory and Practices. CRC Press, Taylor & Francis Group.
4. Ali, M. M., Ibrahim, M. and Yousof, H. M. (2021a). Expanding the Burr X model: properties, copula, real data modeling and different methods of estimation. *Optimal Decision Making in Operations Research & Statistics: Methodologies and Applications*, VOL 1, pp. 21-42.
5. Ali, M. M., Ibrahim, M. and Yousof, H. M. (2022). A New Flexible Three-Parameter Compound Chen Distribution: Properties, Copula and Modeling Relief Times and Minimum Flow Data. *Bulletin of the Malaysian Mathematical Sciences Society*, 45(1), 130-160.
6. Ali, M. M., Yousof, H. M. and Ibrahim, M. (2021b). A new version of the generalized Rayleigh distribution with copula, properties, applications and different methods of estimation. *Optimal Decision Making in Operations Research & Statistics: Methodologies and Applications*, VOL 1, pp. 1-20.
7. Ali, M. M., Yousof, H. M. and Ibrahim, M. (2021). A New Lomax Type Distribution: Properties, Copulas, Applications, Bayesian and Non-Bayesian Estimation Methods. *International Journal of Statistical Sciences*, 21(2), 61-104.
8. Al-babtain, A. A., Elbatal, I. and Yousof, H. M. (2020). A new flexible three-parameter model: properties, Clayton copula, and modeling real data. *Symmetry*, 12(3), pp. 440.
9. Altun, E., Yousof, H. M., Chakraborty, S. and Handique, L. (2018a). Zografos-Balakrishnan Burr $\chi\chi\chi$ distribution: regression modeling and applications. *International Journal of Mathematics and Statistics*, 19(3), 46-70.
10. Altun, E., Yousof, H. M. and Hamedani, G. G. (2018b). A new log-location regression model with influence diagnostics and residual analysis. *Facta Universitatis, Series: Mathematics and Informatics*, 33(3), 417-449.
11. Bjerkedal, T. (1960). Acquisition of resistance in Guinea pigs infected with different doses of virulent tubercle bacilli. *American Journal of Hygiene*, 72, 130–148.
12. Burr, I. W. (1942). Cumulative frequency functions. *Annals of Mathematical Statistics*, 13, 215-232.
13. Burr, I. W. (1968). On a general system of distributions, III.The simplerange. *Journal of the American Statistical Association*, 63, 636-643.
14. Burr, I. W. (1973). Parameters for a general system of distributions to match a grid of 3 and 4. *Communications in Statistics*, 2, 1-21.
15. Burr, I. W. and Cislak, P. J. (1968). On a general system of distributions: I. Its curve-shaped characteristics; II. The sample median. *Journal of the American Statistical Association*, 63, 627-635.
16. Crowder M. J., Kimber A. C., Smith R. L and Sweeting, T. J. (1991). Statistical analysis of reliability data, CHAPMAN & HALL/CRC.
17. Cordeiro, G. M., Yousof, H. M., Ramires, T. G. and Ortega, E. M. M. (2018). The Burr $\chi\chi\chi$ system of densities: properties, regression model and applications. *Journal of Statistical Computation and Simulation*, 88, 432-456.
18. Elgohari, H. and Yousof, H. M. (2020a). A Generalization of Lomax Distribution with Properties, Copula and Real Data Applications. *Pakistan Journal of Statistics and Operation Research*, 16(4), pp. 697-711. <https://doi.org/10.18187/pjsor.v16i4.3260>
19. Elgohari, H. and Yousof, H. M. (2020b). New Extension of Weibull Distribution: Copula, Mathematical Properties and Data Modeling. *Statistics, Optimization & Information Computing*, 8(4), pp. 972-993. <https://doi.org/10.19139/soic-2310-5070-1036>
20. Elsayed, H. A. H. and Yousof, H. M. (2019). The Burr X Nadarajah Haghghi distribution: statistical properties and application to the exceedances of flood peaks data. *Journal of Mathematics and Statistics*, 15, pp. 146-157.
21. Elsayed, H. A. H. and Yousof, H. M. (2021). Extended Poisson Generalized Burr $\chi\chi\chi$ Distribution. *Journal of Applied Probability and Statistics*, 16(1), 1-30.
22. Gumbel, E. J. (1960). Bivariate exponential distributions. *Journal of the American Statistical Association*, 55, pp. 698-707.
23. Gumbel, E. J. (1961). Bivariate logistic distributions. *Journal of the American Statistical Association*, 56, pp. 335-349.
24. Gad, A. M., Hamedani, G. G., Salehabadi, S. M. and Yousof, H. M. (2019). The Burr $\chi\chi\chi$ -Burr $\chi\chi\chi$ distribution: mathematical properties and characterizations. *Pakistan Journal of Statistics*, 35(3), 229-248.
25. Gijbels, I. and Gürler, U. (2003). Estimation of a change point in a hazard function based on censored data. *Lifetime Data Analysis*, 9(4), 395-411.
26. Korkmaz, M. C., Yousof, H. M., Rasekhi, M. and Hamedani, G. G. (2018). The Odd Lindley Burr $\chi\chi\chi$ Model: Bayesian Analysis, Classical Inference and Characterizations. *Journal of Data Science*, 16(2), 327-353.
27. Mansour, M. M., Ibrahim, M., Aidi, K., Shafique Butt, N., Ali, M. M., Yousof, H. M. and Hamed, M. S. (2020a). A New Log-Logistic Lifetime Model with Mathematical Properties, Copula, Modified Goodness-of-Fit Test for Validation and Real Data Modeling. *Mathematics*, 8(9), pp. 1508.
28. Mansour, M. M., Butt, N. S., Ansari, S. I., Yousof, H. M., Ali, M. M. and Ibrahim, M. (2020b). A new exponentiated Weibull distribution's extension: copula, mathematical properties and applications. *Contributions to Mathematics*, 1 (2020), pp. 57-66.
29. Mansour, M., Korkmaz, M. C., Ali, M. M., Yousof, H. M., Ansari, S. I. and Ibrahim, M. (2020c). A generalization of the exponentiated Weibull model with properties, Copula and application. *Eurasian Bulletin of Mathematics*, 3(2), pp.

- 84-102.
30. Mansour, M., Rasekhi, M., Ibrahim, M., Aidi, K., Yousof, H. M. and Elrazik, E. A. (2020d). A New Parametric Life Distribution with Modified Bagdonavičius–Nikulin Goodness-of-Fit Test for Censored Validation, Properties, Applications, and Different Estimation Methods. *Entropy*, 22(5), pp. 592.
 31. Mansour, M., Yousof, H. M., Shehata, W. A. and Ibrahim, M. (2020e). A new two parameter Burr \mathcal{XII} distribution: properties, copula, different estimation methods and modeling acute bone cancer data. *Journal of Nonlinear Science and Applications*, 13(5), pp. 223-238.
 32. Mansour, M. M., Butt, N. S., Yousof, H. M., Ansari, S. I. and Ibrahim, M. (2020f). A Generalization of Reciprocal Exponential Model: Clayton Copula, Statistical Properties and Modeling Skewed and Symmetric Real datasets. *Pakistan Journal of Statistics and Operation Research*, 16(2), pp. 373-386.
 33. Morgenstern, D. (1956). Einfache beispiele zweidimensionaler verteilungen. *Mitteilungsblattfur Mathematische Statistik*, 8, pp. 234-235.
 34. Pougaza, D. B. and Djafari, M. A. (2011). Maximum entropies copulas. Proceedings of the 30th international workshop on Bayesian inference and maximum. *Entropy methods in Science and Engineering*, pp. 329-336.
 35. Rasekhi, M., Saber, M. M., & Yousof, H. M. (2020). Bayesian and classical inference of reliability in multicomponent stress-strength under the generalized logistic model. *Communications in Statistics-Theory and Methods*, 50(21), 5114-5125.
 36. Rodriguez-Lallena, J. A. and Ubeda-Flores, M. (2004). A new class of bivariate copulas. *Statistics and Probability Letters*, 66, pp. 315-25.
 37. Saber, M. M. and Yousof, H. M. (2022). Bayesian and Classical Inference for Generalized Stress-strength Parameter under Generalized Logistic Distribution, *Statistics, Optimization & Information Computing*, forthcoming.
 38. Saber, M. M. Marwa M. Mohie El-Din and Yousof, H. M. (2022). Reliability estimation for the remained stress-strength model under the generalized exponential lifetime distribution, *Journal of Probability and Statistics*, 2021, 1-10.
 39. Saber, M. M., Rasekhi, M. and Yousof, H. M. (2022). Generalized Stress-Strength and Generalized Multicomponent Stress-Strength Models, *Statistics, Optimization & Information Computing*, forthcoming.
 40. Nichols, M. D. and Padgett, W. J. (2006). A bootstrap control chart for Weibull percentiles. *Quality and reliability engineering international*, 22, 141-151.
 41. Paranaíba, P. F. P., Ortega, E. M. M., Cordeiro, G. M. and de Pascoa, M. A. R. (2013). The Kumaraswamy Burr \mathcal{XII} distribution: theory and practice. *Journal of Statistical Computation and Simulation*, 83, 2117-2143.
 42. Paranaíba, P. F. P., Ortega, E. M. M., Cordeiro, G. M. and Pescim, R. R. (2011). The beta Burr \mathcal{XII} distribution with application to lifetime data. *Computation Statistics and Data Analysis*, 55, 1118-1136.
 43. Rodriguez, R.N. (1977). A guide to the Burr type- \mathcal{XII} distributions. *Biometrika*, 64, 129-134.
 44. Shehata, W. A. M. and Yousof, H. M. (2022). A novel two-parameter Nadarajah-Haghighi extension: properties, copulas, modeling real data and different estimation methods. *Statistics, Optimization & Information Computing*, 10(3), 725-749.
 45. Shehata, W. A. M. and Yousof, H. M. (2021). The four-parameter exponentiated Weibull model with Copula, properties and real data modeling. *Pakistan Journal of Statistics and Operation Research*, 17(3), 649-667.
 46. Shehata, W. A. M., Yousof, H. M., & Aboraya, M. (2021). A Novel Generator of Continuous Probability Distributions for the Asymmetric Left-skewed Bimodal Real-life Data with Properties and Copulas . *Pakistan Journal of Statistics and Operation Research*, 17(4), 943-961. <https://doi.org/10.18187/pjsor.v17i4.3903>
 47. Shehata, W. A. M., Butt, N. S., Yousof, H., & Aboraya, M. (2022). A New Lifetime Parametric Model for the Survival and Relief Times with Copulas and Properties. *Pakistan Journal of Statistics and Operation Research*, 18(1), 249-272.
 48. Sickle-Santanello, B.J, Farrar, W. B, Decenzo, J. F, Keyhani-Rofagha, S, Klein, J, Pearl, D, Laufman, H, O'Toole, R.V. (1988). Technical and statistical improvements for flow cytometric DNA analysis of para n-embedded tissue. *Cytometry*, 9(6), 954-599.
 49. Tadikamalla, P. R. (1980). A look at the Burr and related distributions, *International Statistical Review*, 48, 337-344.
 50. Yousof, H. M., Ahsanullah, M. and Khalil, M. G. (2019a). A new zero-truncated version of the Poisson Burr \mathcal{XII} distribution: Characterizations and properties. *Journal of Statistical Theory and Applications*, 18(1), 1-11.
 51. Yousof, H. M., Altun, E., Ramires, T. G., Alizadeh, M. and Rasekhi, M. (2018). A new family of distributions with properties, regression models and applications, *Journal of Statistics and Management Systems*, 21, 163-188.
 52. Yousof, H. M., Rasekhi, M., Altun, E., Alizadeh, M. Hamedani G. G. and Ali M. M. (2019b). A new lifetime model with regression models, characterizations and applications. *Communications in Statistics-Simulation and Computation*, 48(1), 264-286.
 53. Yousof, H. M. and Korkmaz, M. C. (2017). Topp-Leone Nadarajah-Haghighi distribution: mathematical properties and applications, *International Journal of Applied Mathematics*. *Journal of Statisticians: Statistics and Actuarial Sciences*, 2, pp. 119-128.
 54. Yousof, H. M., Hamedani, G. G. and Ibrahim, M. (2020). The Two-parameter Xgamma Fréchet Distribution: Characterizations, Copulas, Mathematical Properties and Different Classical Estimation Methods. *Contributions to Mathematics*, 2, 32-43.
 55. Yousof, H. M., Korkmaz, M. C. Hamedani G. G. (2017). The odd Lindley Nadarajah-Haghighi distribution. *J. Math. Comput. Sci.*, 7, pp. 864-882.